Phys Chem Minerals (2001) 28: 302–312

ORIGINAL PAPER

H. Xu · P. J. Heaney · A. Navrotsky

Thermal expansion and structural transformations of stuffed derivatives of quartz along the $LiAlSiO_4$–SiO_2 join: a variable-temperature powder synchrotron XRD study

Received: 26 June 2000 / Accepted: 1 December 2000

Abstract The structural behavior of stuffed derivatives of quartz within the $Li_{1-x}Al_{1-x}Si_{1+x}O_4$ system ($0 \le x \le 1$) has been studied in the temperature range 20 to 873 K using high-resolution powder synchrotron X-ray diffraction (XRD). Rietveld analysis reveals three distinct regimes whose boundaries are defined by an Al/Si order-disorder transition at $x = \sim 0.3$ and a β–α displacive transformation at $x = \sim 0.65$. Compounds that are topologically identical to β-quartz ($0 \le x < \sim 0.65$) expand within the (0 0 1) plane and contract along c with increasing temperature; however, this thermal anisotropy is significantly higher for structures within the regime $0 \le x < \sim 0.3$ than for those with compositions $\sim 0.3 \le x < \sim 0.65$. We attribute this disparity to a tetrahedral tilting mechanism that occurs only in the ordered structures ($0 \le x < \sim 0.3$). The phases with $\sim 0.65 \le x \le 1$ adopt the α-quartz structure at room temperature, and they display positive thermal expansion along both a and c from 20 K to their α–β transition temperatures. This behavior arises mainly from a rotation of rigid Si(Al)-tetrahedra about the $\langle 100 \rangle$ axes. Landau analysis provides quantitative evidence that the charge-coupled substitution of Li + Al for Si in quartz dampens the α–β transition. With increasing Li + Al content, the low-temperature modifications exhibit a marked decrease in spontaneous strain; this behavior reflects a weakening of the first-order character of the transition. In addition, we observe a linear decrease in the α–β critical temperature from 846 K to near 0 K as the Li + Al content increases from $x = 0$ to $x = \sim 0.5$.

Key words Thermal expansion · Phase transition · β-Eucryptite · Quartz · X-ray diffraction

H. Xu (✉)
Department of Geosciences and Princeton Materials Institute, Princeton University, Princeton, New Jersey 08544, USA

P. J. Heaney
Department of Geosciences, The Pennsylvania State University, University Park, Pennsylvania 16802, USA

A. Navrotsky
Department of Chemical Engineering and Materials Science, University of California at Davis, Davis, California 95616, USA

Present address:
H. Xu, Department of Chemical Engineering and Materials Science, University of California at Davis, Davis, California 95616, USA
Tel.: +1-530-754-2132; Fax: +1-530-752-9307
e-mail: hxu@ucdavis.edu

Introduction

As one of the most compact framework structures, quartz is not very tolerant of interstitial substitutions. Nevertheless, small cations such as Li^+ and Mg^{2+} can occupy tunnel sites in the quartz framework, and charge neutrality is achieved by replacing a fraction of the Si^{4+} cations with cations having lower valences, such as Al^{3+} and B^{3+} (Buerger 1954; Palmer 1994; Müller 1995). This charge-coupled substitution mechanism produces a family of materials that Buerger (1954) classified as the "stuffed derivatives of quartz."

Stuffed quartz-derivative phases having the composition $Li_{1-x}Al_{1-x}Si_{1+x}O_4$ with $0 \le x \le 1$ belong to the so-called LAS (Li_2O–Al_2O_3–SiO_2) ternary system, one of the most extensively studied and utilized groups of glass-ceramic materials (Beall 1994; Roy 1995). Depending on the concentrations of substitutional $Li^+ + Al^{3+}$, these phases can crystallize in either the β-quartz ($0 \le x < \sim 0.65$) or the α-quartz ($\sim 0.65 \le x \le 1$) structures (Xu et al. 2000). Much of the interest in this group of materials has focused on the β-quartz derivatives, because they possess near-zero coefficients of thermal expansion (CTE). For example, the end-member β-eucryptite ($LiAlSiO_4$) has long been known to maintain a nearly constant volume from room temperature to 1473 K (Schulz 1974); on heating, the volume change produced by expansion within the (0 0 1) plane is approximately canceled by contraction along the c-axis (e.g., Schulz 1974; Xu et al. 1999a). As a result,

these materials are common components of high-temperature glass-ceramic products used in domestic cookware and in many high-precision machines such as jet engines (Beall 1994).

The thermal behavior of end-member β-eucryptite has been intensively studied (e.g., Gillery and Bush 1959; Pillars and Peacor 1973; Schulz 1974; Müller 1995). In our recent examination of β-eucryptite, we monitored thermal expansion behavior from 20 to 873 K by combined synchrotron X-ray and neutron diffraction (Lichtenstein et al. 1998; Xu et al. 1999a). We found that the near-zero thermal expansion of β-eucryptite persists to low temperatures, and we proposed that this isovolumetric behavior results from several interdependent processes, including tetrahedral tilting, tetrahedral deformation, and Li positional disordering.

Despite the attention paid to end-member β-eucryptite, only a few investigations have extended to intermediate compositions along the $LiAlSiO_4$–SiO_2 join. Petzoldt (1967) argued from dilatometric measurements that end-member β-eucryptite exhibits a negative coefficient of thermal expansion over the temperature range 293 to 573 K, but the CTEs of β-quartz solid solutions become less negative with increasing silica content up to 55 wt% SiO_2 ($Li_{0.85}Al_{0.85}Si_{1.15}O_4$). Petzoldt also suggested that at higher silica concentrations, thermal expansion coefficients are roughly equal. However, more recent high-temperature X-ray diffraction studies indicate that the CTE for the composition $Li_{0.67}Al_{0.67}Si_{1.33}O_4$ (-2.1×10^{-6}/K; Müller et al. 1988) is more negative than that for $LiAlSiO_4$ (-0.4×10^{-6}/K; Pillars and Peacor 1973). The inconsistency of these few data illustrates the need for a more systematic study of the thermal expansion behavior over the entire series.

It is not surprising that stuffed derivatives of α-quartz in the $Li_{1-x}Al_{1-x}Si_{1+x}O_4$ system have received less scrutiny, simply because they do not possess the low CTEs exhibited by the β-quartz derivatives. However, since α-quartz structures undergo phase transitions to β-quartz on heating, the stuffed α-quartz phases constitute an ideal system for systematically investigating the effects that charge-coupled substitutions exert on transition behavior. Because the α–β quartz transformation is one of the most exhaustively studied displacive transitions (see review by Heaney and Veblen 1991a), this study may provide insights into the general ways in which impurities induce morphotropic phase transitions (Heaney 2000).

Impurities have been found to radically modify the behavior of phase transitions in many systems (e.g., Salje 1990; Salje et al. 1991; Redfern 1992; Carpenter 1992). Though the specific effects of impurities are individual to a given structure and defect mechanism, manifestations of impurities that are shared among various minerals would include: (1) an increase or decrease in the critical temperature; (2) a temperature-broadening of the transition event; and (3) a decrease in the mobility of transition-induced domain boundaries. For example, several authors have shown that the critical temperature of the α–β quartz transition decreases with an increased $M^+ + Al^{3+}$ substitution for Si^{4+} ($M^+ = Li^+$, Na^+, K^+ and H^+) (Keith and Tuttle 1952; Smith and Steele 1984). Moreover, point defects, such as interstitial cations, appear responsible for memory effects in quartz by pinning Dauphiné twin boundary positions (Heaney and Veblen 1991b; Xu and Heaney 1997). However, systematic studies of the impact of impurities on displacive transitions in silicates are relatively rare, and predicting the crystallographic changes that impurities will impose on framework structures remains an inexact science.

In the present investigation, five samples with the compositions $Li_{1-x}Al_{1-x}Si_{1+x}O_4$, $x = 0.2$, 0.33, 0.5, 0.69, and 0.9, were examined by powder synchrotron X-ray diffraction from 20 to 873 K. Rietveld analyses of the data have allowed high-precision determinations of unit-cell parameters as a function of temperature. By incorporating these results with those for end-member β-eucryptite (Xu et al. 1999a), we present a full structural explanation for the thermal behavior of the $LiAlSiO_4$–SiO_2 system. In addition, we have quantified the weakening of the first-order character of the α–β transition by measuring the critical temperatures and spontaneous strains associated with the α–β inversions for the stuffed derivatives of α-quartz with increasing Li + Al substitution for Si.

Crystallographic background

The structure of β-quartz, the high-temperature polymorph of quartz above 846 K consists of paired helical chains of silica tetrahedra that produce open channels parallel to c (e.g., Heaney 1994). Within the channels, distorted tetrahedral and octahedral cavities alternate along c, and these cavities can accommodate small cations such as Li^+ and Mg^{2+} (Schulz 1974; Palmer 1994). Pure β-quartz displacively transforms to denser α-quartz on cooling with a concomitant space group change from $P6_222$ or $P6_422$ to $P3_221$ or $P3_121$. However, stuffing small cations into the channel sites can buttress the framework from collapse and stabilize the β-quartz structure at room temperature (Beall 1994).

The fully stuffed lithian derivative of β-quartz is stoichiometric β-eucryptite, $LiAlSiO_4$. Previous structure analyses (e.g., Tscherry et al. 1972; Pillars and Peacor 1973; Müller 1979; Xu et al. 1999b) have revealed that β-eucryptite has doubled translational periodicities along c and a relative to β-quartz (Fig. 1a). This superstructure arises from the ordering of Al and Si ions in alternate layers normal to c with collateral ordering of Li within two distinct channels. However, as silica content increases in the $Li_{1-x}Al_{1-x}Si_{1+x}O_4$ series, the superstructure is gradually lost and disappears at $x = \sim 0.3$ (Fig. 1b) as the result of an Al/Si disordering transition at this composition (Xu et al. 1999a).

With less than ~35 mol% substitution of Li + Al for Si ($x \geq \sim 0.65$), the $Li_{1-x}Al_{1-x}Si_{1+x}O_4$ compounds cannot maintain the β-quartz structure, since Li concen-

tration is not sufficient to hold open the expanded framework (Petzoldt 1967; Xu et al. 2000). Rather, these more siliceous compositions adopt the α-quartz modification (Fig. 1c). Therefore, the $Li_{1-x}Al_{1-x}Si_{1+x}O_4$ solid solution series is divided into three distinct structural regimes: (1) $0 \le x < \sim 0.3$; (2) $\sim 0.3 \le x < \sim 0.65$; and (3) $\sim 0.65 \le x \le 1$. Variations of unit-cell parameters as a function of composition exhibit abrupt changes in slope at the boundaries of these three regimes (Xu et al. 2000).

Experimental methods

Sample synthesis

Stuffed quartz-derivative phases with compositions $Li_{1-x}Al_{1-x}Si_{1+x}O_4$, $x = 0.2$, 0.33, 0.5, 0.69, and 0.9, were prepared for this study. Because these phases exhibit different regions of thermodynamic stability and metastability, three synthesis methods were employed: (1) high-temperature sintering for $x = 0.2$; (2) high-pressure high-temperature processing for $x = 0.33$, 0.5, and 0.9; and (3) glass annealing for $x = 0.69$. Detailed synthesis and sample characterization procedures have been described in Xu et al. (1999c). As noted in Xu et al. (1999c), the samples with $x = 0.2$, 0.33, and 0.69 are single phases consistent with their nominal compositions, whereas those with $x = 0.5$ and 0.9 contain two intergrown phases (weight fractions: 84/16 for $x = 0.5$ and 64/36 for $x = 0.9$) with slightly different compositions.

X-ray diffraction data collection

Powder X-ray diffraction measurements were performed using two instruments. All low-temperature experiments and most high-temperature experiments were carried out with a linear position-sensitive detector (PSD) at beam line X7A (Cox et al. 1988) of the National Synchrotron Light Source (NSLS), Brookhaven National Laboratory (BNL). The wavelengths used ranged from 0.7 to 0.8 Å, as calibrated using a CeO_2 standard. Diffraction data were collected for the following temperatures: 20, 100, 200, 298, 543, 748, and 873 K for all samples, and several additional temperatures, 60, 150, 225, 250, and 275 K, for the $Li_{0.31}Al_{0.31}Si_{1.69}O_4$ phase only. For high-temperature experiments, the powder samples were sealed in 0.2-mm diameter quartz-glass capillaries, and the capillaries were mounted in a furnace consisting of a 1.25-inch diameter wire-wound BN tube and outer water-cooled Al tube. For low-temperature measurements, the samples were sealed in silica-glass capillaries of 0.2-mm diameter, and the capillaries were placed in a cryogenic displex cooled by helium in a two-stage closed-cycle refrigerator. Sample temperatures were registered with a Chromel-Alumel thermocouple positioned just below the center of the capillary, and they were found to be stable within 1 K. In order to minimize preferred orientation, the sample capillaries were fully rotated during the high-T data collection and were rocked through ± 10° during the low-T data collection. Data were collected from 7 to 55° 2θ in step scan mode using steps of 0.25° with counting times of 10 s (7–15°), 20 s (15–30°), 40 s (30–45°), and 80 s (45–55°) per step.

To obtain additional data for Landau analysis of the $Li_{0.31}Al_{0.31}Si_{1.69}O_4$ phase, high-temperature experiments were performed with a Scintag PAD-V theta-theta diffractometer using CuKα radiation and a scintillation detector. The temperatures ranged from 313 to 773 K with intervals of 20 K. A thin layer of the sample powder was mounted on a Pt resistance-strip heating stage, and the temperatures were measured with a Pt-$Pt_{87}Rh_{13}$ thermocouple. Data were collected from 15 to 100° 2θ in step scan mode with steps of 0.03° and count times of 4 s per step.

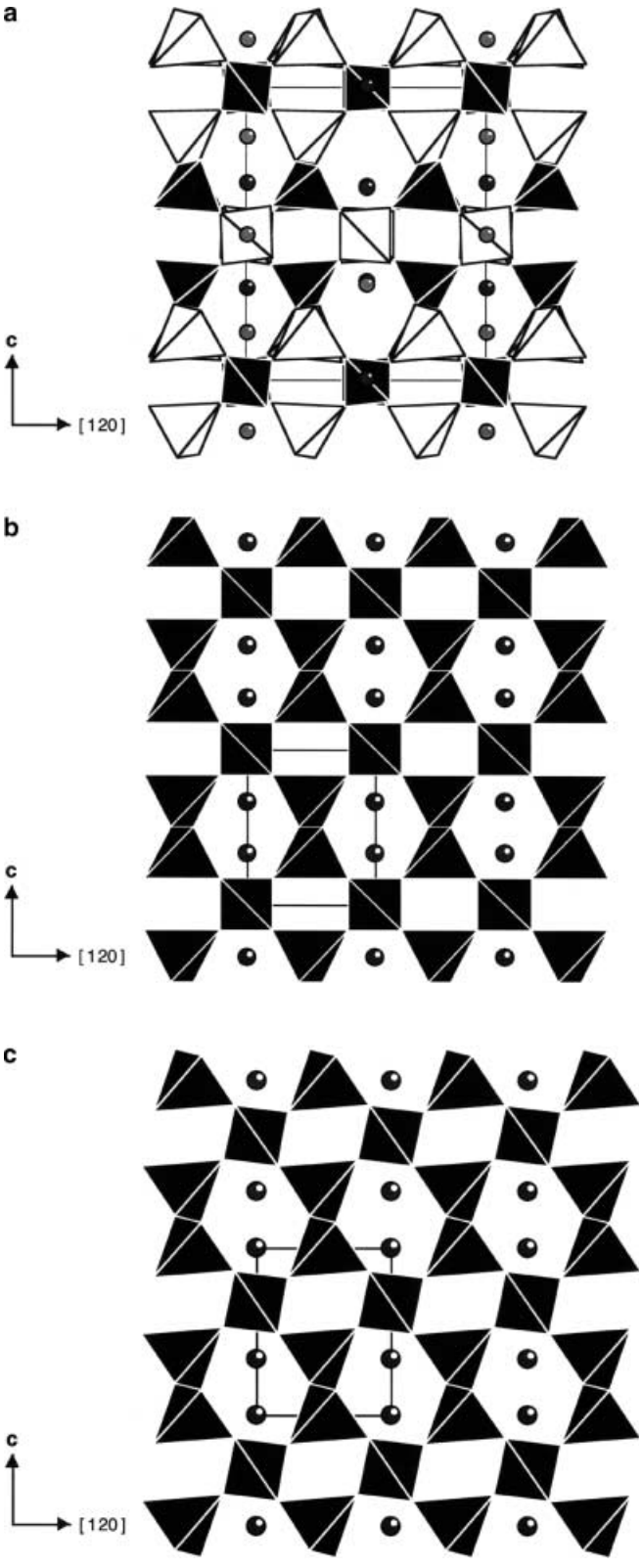

Fig. 1a–c The structures for the $Li_{1-x}Al_{1-x}Si_{1+x}O_4$ phases projected along the **a**-axis. **a** $x = 0$ **b** $x = 0.33$ **c** $x = 0.69$. *Spheres* represent Li ions. Si- and Al-tetrahedra are plotted in *black and white*, respectively, in the ordered structure in **a**. In **b** and **c**, Si and Al are disordered and all tetrahedra are plotted in *black*. *Light lines* outline the unit cell

Structure refinements

Rietveld refinements for the $Li_{1-x}Al_{1-x}Si_{1+x}O_4$ compounds were performed using the general structure analysis system (GSAS) program of Larson and Von Dreele (1994). Depending on the composition, the starting atomic parameters in our first refinements of the room temperature structures were taken from the following studies: for $x = 0.2$, the study of β-eucryptite (space group $P6_222$) by Guth and Heger (1979); for $x = 0.33$ and 0.5, the study of $Li_{0.67}Al_{0.67}Si_{1.33}O_4$ (space group $P6_222$) by Li (1968); and for $x = 0.69$ and 0.9, the study of α-quartz (space group $P3_221$) by Will et al. (1988). We then used our room-temperature results for the starting structures at the next-nearest temperatures and continued this procedure systematically with changing temperature. Since the stuffed α-quartz-derivative phases ($x = 0.69$ and 0.9) transform to their β modifications at high temperatures, we used the structure model of β-quartz (Wright and Lehman, 1981) in the refinements of those high-temperature structures. Likewise, the β-quartz-derivative phases in the sample with $x = 0.5$ undergo transitions to the α-quartz-like polymorphs on cooling, and thus some of these low-temperature structures were refined based on the model of α-quartz (Will et al. 1988).

Our refinements proceeded as follows: after scale factor and four RDF (radial distribution function, needed for modeling the background from the glass capillary) background terms for each histogram had converged, specimen displacement and lattice parameters were added and optimized. Between two and ten additional background terms were then added for each histogram, and the peak profiles were fitted by refining isotropic and anisotropic Lorentzian broadening parameters and a Gaussian particle size coefficient in a pseudo-Voigt function (Thompson et al. 1987; Finger et al. 1994). Upon convergence of the above parameters, atomic positions and isotropic temperature factors for Li, Al, Si, and O were refined (except for the analysis of conventional X-ray data of $Li_{0.31}Al_{0.31}Si_{1.69}O_4$). For the binary samples with $x = 0.5$ and 0.9, we refined the weight fractions of their two co-existing phases with the constraint that the individual weight fractions sum to unity.

Differential scanning calorimetry

To determine the α–β transition temperatures for the stuffed derivatives of α-quartz with compositions $Li_{1-x}Al_{1-x}Si_{1+x}O_4$, $x = 0.69$ and 0.9, differential scanning calorimetry (DSC) was performed using a Netzsch 404 high-temperature calorimeter. Sample powders of ~55 mg were tightly packed in a Pt crucible, and the data were collected over the temperature range 303–963 K with a scan rate of 10 K min^{-1}. Temperature was calibrated against the known melting points of several metals by the manufacturer. In addition, our DSC analysis of an end-member quartz sample (Fluka-Garantie) revealed an endothermic peak arising from the α–β quartz transition at 845.4 K, in good agreement with the well-accepted value of 846 K (e.g., Zeyen et al. 1983), thereby confirming the accuracy of the temperature calibration.

Results and discussion

Thermal expansion behavior

Unit-cell parameters

The temperature dependence of the lattice parameters for the $Li_{1-x}Al_{1-x}Si_{1+x}O_4$ phases with $x = 0.2$, 0.33, 0.5, 0.69, and 0.9, are presented in Table 1 and Figs. 2 and 3, together with the data for the two end members of the series, β-eucryptite and α-quartz, for comparison. As shown in Fig. 2a and b, the thermal behavior of the stuffed derivatives of β-quartz ($x = 0.2$, 0.33, and 0.5) is similar to that of β-eucryptite: with increasing temperature, c decreases while a remains approximately unchanged up to 298 K and increases thereafter. Likewise, the volume thermal expansion for these compounds is slightly negative below room temperature and near-zero at high temperatures (Fig. 2c). However, as silica content increases, the degree of variation in a and c becomes significantly smaller. In other words, the anisotropy of thermal expansion decreases with increasing x. This trend is consistent with previous measurements showing that the absolute values of axial CTEs for $LiAlSiO_4$ ($\alpha_a = 8.6 \times 10^{-6}\ K^{-1}$, $\alpha_c = -18.4 \times 10^{-6}\ K^{-1}$; Pillars and Peacor 1973) are larger than the corresponding values for the more siliceous $Li_{0.67}Al_{0.67}Si_{1.33}O_4$ ($\alpha_a = 1.0 \times 10^{-6}\ K^{-1}$, $\alpha_c = -6.3 \times 10^{-6}\ K^{-1}$; Müller et al. 1988).

As expected, the stuffed α-quartz-derivative phases ($x = 0.69$ and 0.9) displacively transform to β-quartz-like structures on heating. Consequently, variations of lattice parameters with temperature for these phases show sharp changes in slope at their critical temperatures (Fig. 3a–c). Just as in pure quartz, with increasing temperature the a- and c-axes for both phases expand at an increasing rate up to the critical point, and then a remains constant while c decreases. However, the c-axis contraction of the β form is much steeper for $x = 0.69$ than for $x = 0.9$ and pure quartz. In addition, the critical temperature shifts to lower values (e.g., 344 K for $x = 0.69$ in comparison with 846 K for pure quartz) with higher Li + Al substitution.

Since those LAS compounds that adopt the α-quartz configuration at room temperature displacively transform to β-quartz-like modifications with high temperature, it is reasonable to expect that some LAS compounds that are isostructural with β-quartz at room temperature will displacively transform to α-quartz-like modifications on cooling. As shown in Fig. 4a and b, the secondary phase (representing ~16 wt%) in the sample with bulk composition $x = 0.5$ exhibits a rapid decrease in lattice parameters when the temperature drops from 200 to 100 K. We interpret this behavior as evidence for a β-to-α quartz-like transition for this secondary phase below room temperature, as has not been previously described for compounds within the $Li_{1-x}Al_{1-x}Si_{1+x}O_4$ system.

Structural variations

In a separate variable-temperature diffraction study of end-member β-eucryptite (Xu et al. 1999a), we demonstrated that thermal expansion is related to three interconnected processes: tetrahedral tilting; tetrahedral deformation; and Li disordering. All of these transformation mechanisms can cause an extension of the structure in the (0 0 1) plane and a contraction along the c-axis with increasing temperature. Moreover, we observed that β-eucryptite with complete cation (Al/Si and Li) disorder is much less anisotropic in its thermal

Table 1 Unit-cell parameters for stuffed quartz-derivative phases $Li_{1-x}Al_{1-x}Si_{1+x}O_4$ as a function of temperature (determined from synchroton X-ray data)[a]

T (K)	a ($x=0$)[b]	c ($x=0$)[b]	V ($x=0$)[b]	a ($x=0.20$)	c ($x=0.20$)	V ($x=0.20$)	a ($x=0.33$)	c ($x=0.33$)	V ($x=0.33$)
20	5.2453(1)	5.6145(1)	133.778(3)	5.2467(1)	5.5001(2)	131.119(8)	5.2122(1)	5.4696(1)	128.684(3)
100	5.2451(1)	5.6120(1)	133.710(3)	5.2460(1)	5.4970(2)	131.009(8)	5.2114(1)	5.4673(1)	128.588(4)
200	5.2458(1)	5.6049(1)	133.569(4)	5.2460(1)	5.4906(2)	130.855(8)	5.2104(1)	5.4616(1)	128.410(4)
250	5.2468(1)	5.6017(1)	133.547(3)						
298	5.2481(1)	5.5978(1)	133.525(5)	5.2472(1)	5.4825(2)	130.725(8)	5.2102(1)	5.4551(1)	128.242(4)
523	5.2541(1)	5.5779(1)	133.351(4)	5.2504(3)	5.4685(4)	130.551(20)	5.2158(1)	5.4475(1)	128.340(7)
636	5.2586(1)	5.5680(1)	133.341(5)						
748	5.2634(1)	5.5568(1)	133.317(5)	5.2571(3)	5.4576(4)	130.621(18)	5.2167(1)	5.4390(2)	128.190(8)
873	5.2701(1)	5.5450(1)	133.373(5)	5.2603(3)	5.4530(4)	130.673(18)	5.2174(2)	5.43577(2)	128.144(9)
	a ($x=0.50$)[c]	c ($x=0.50$)[c]	V ($x=0.50$)[c]	a ($x=0.69$)	c ($x=0.69$)	V ($x=0.69$)	a ($x=0.90$)[c]	c ($x=0.90$)[c]	V ($x=0.90$)[c]
20	5.1647(2)	5.4658(2)	126.261(10)	5.0570(1)	5.4345(1)	120.357(3)	4.9524(2)	5.4112(2)	114.937(11)
60				5.0585(1)	5.4353(1)	120.449(3)			
100	5.1658(2)	5.4659(2)	126.318(12)	5.0600(1)	5.4352(1)	120.519(3)	4.9534(2)	5.4114(2)	114.985(9)
150				5.0640(1)	5.4362(1)	120.729(3)			
200	5.1655(2)	5.4619(1)	126.210(8)	5.0687(1)	5.4375(1)	120.983(3)	4.9586(2)	5.4138(1)	115.278(7)
225				5.0713(1)	5.4378(1)	121.113(3)			
250				5.0748(1)	5.4390(1)	121.297(3)			
275				5.0789(1)	5.4404(1)	121.533(3)			
298	5.1651(1)	5.4571(1)	126.082(7)	5.0865(1)	5.4451(1)	122.004(3)	4.9672(2)	5.4187(1)	115.783(8)
523	5.1682(3)	5.4506(2)	126.080(14)	5.1105(1)	5.4508(2)	123.286(7)	4.9882(2)	5.4277(2)	116.958(9)
598							5.0065(4)	5.4392(3)	118.068(19)
673							5.0324(6)	5.4476(7)	119.478(36)
748	5.1687(3)	5.4437(2)	125.947(15)	5.1099(1)	5.4454(2)	123.135(7)	5.0317(4)	5.4505(5)	119.510(25)
873	5.1699(3)	5.4426(2)	125.981(13)	5.1074(2)	5.4408(2)	122.913(9)	5.0308(3)	5.4488(3)	119.424(16)

[a] The units: a or c in Å; V in Å^3
[b] From Xu et al. (1999b)
[c] Only results for the major phase of the biphasic mixture are listed here

Fig. 2a–c Effects of temperature and composition on the unit-cell parameters **a** a, **b** c, and **c** V of the stuffed derivatives of β-quartz, $Li_{1-x}Al_{1-x}Si_{1+x}O_4$. For the biphasic mixtures with $x = 0.5$ and 0.9, only the data of the major phases are plotted

expansion than ordered β-eucryptite, and we proposed that the diminished anisotropy in disordered β-eucryptite can be ascribed to the absence of tetrahedral tilting, which occurs only in the ordered structure.

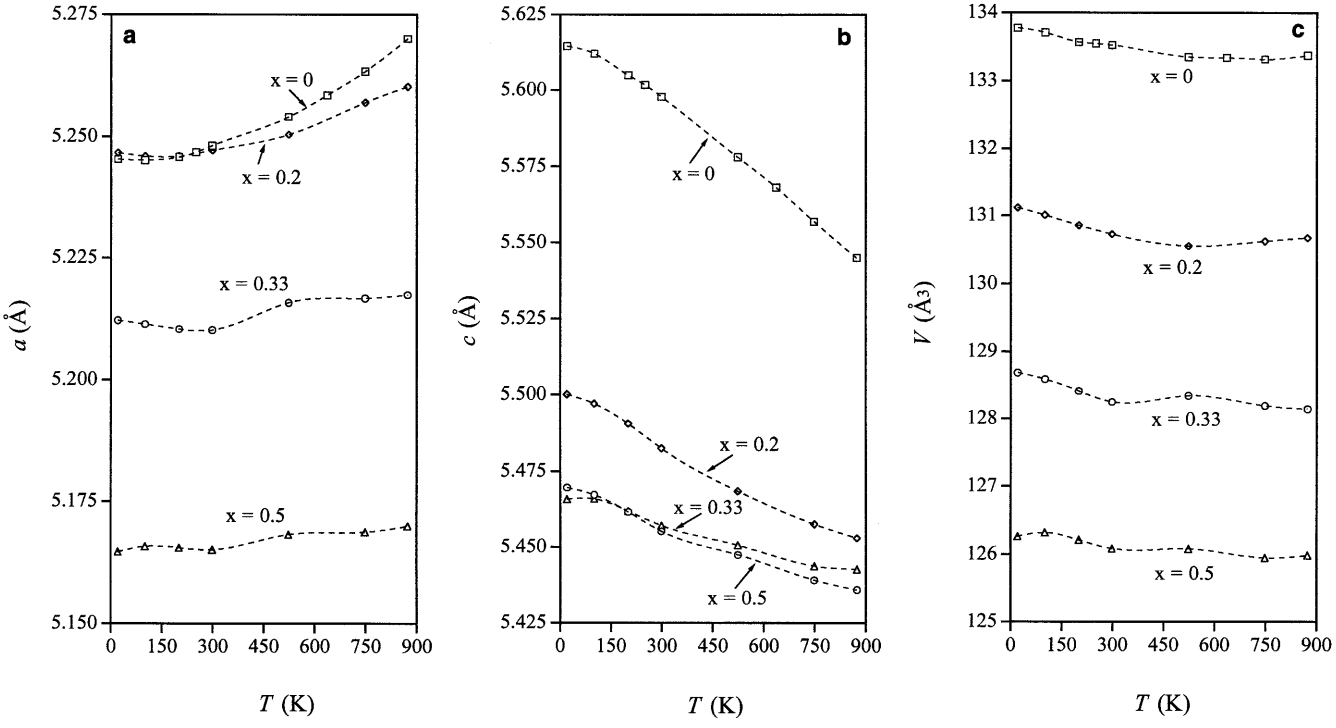

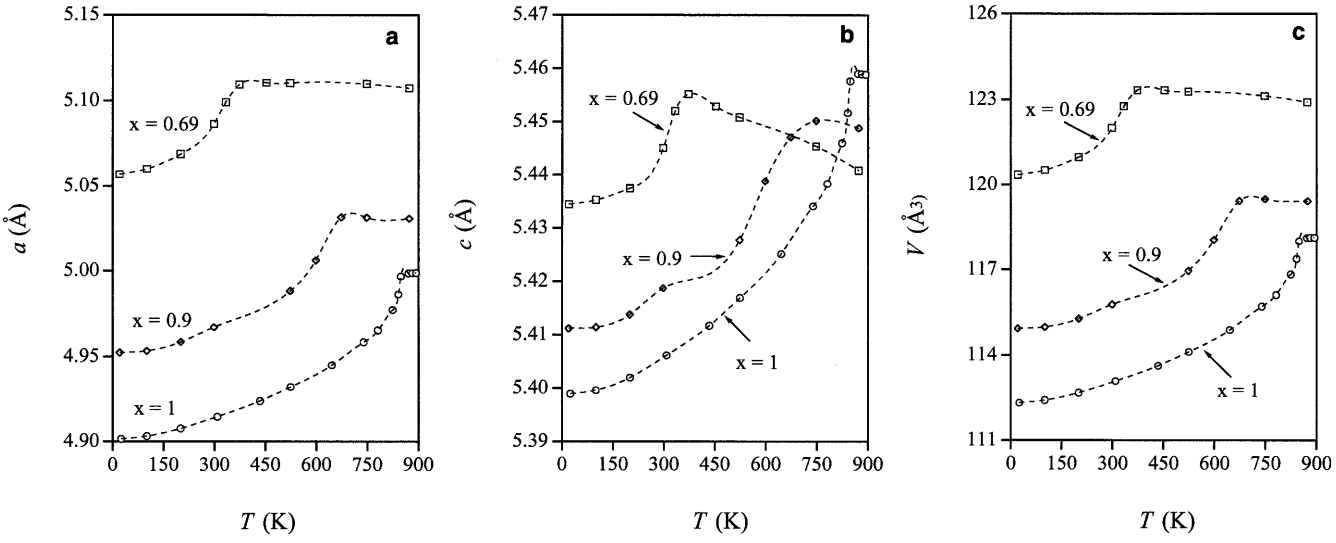

Fig. 3a–c Effects of temperature and composition on the unit-cell parameters **a** a, **b** c, and **c** V of the stuffed derivatives of α-quartz, $Li_{1-x}Al_{1-x}Si_{1+x}O_4$. (Data for pure α-quartz from Carpenter et al. 1998a)

The thermal behavior of the stuffed derivatives of β-quartz with intermediate compositions ($x = 0.2$, 0.33 and 0.5) is controlled by the three transformation mechanisms operative in end-member β-eucryptite. As described in Xu et al. (2000), compositional variations affect the LAS derivatives of quartz in a fashion that parallels changes in temperature. Specifically, with increasing silica concentration, the long-range order of Al and Si progressively diminishes between $x = 0$ and $x = \sim 0.3$, and the structure is fully disordered for $x \geq \sim 0.3$. Because Al/Si order and Li positional order are coupled, the distribution of Li ions over the tetrahedral channel sites also undergoes an order-disorder transition at $x = \sim 0.3$. Thus, the degree of tetrahedral tilting becomes smaller as x increases from 0 to 0.3, and the magnitude of axial thermal expansion along both a and c drops sharply from $x = 0$ to $x = 0.33$ (Fig. 2a, b). This behavior parallels the smaller thermal expansion observed in disordered β-eucryptite in comparison with the ordered end-member (Xu et al. 1999a).

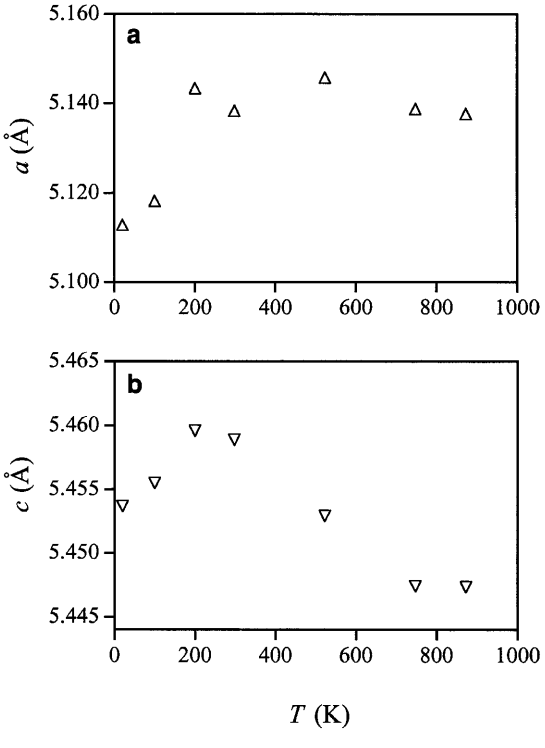

Fig. 4a, b Variation of the unit-cell parameters for the secondary phase (with a weight fraction of ~16%) in the $Li_{0.5}Al_{0.5}Si_{1.5}O_4$ sample as a function of temperature. **a** a-axis and **b** c-axis. The composition of this phase is estimated as $x = \sim 0.58$ based on the variation of cell volume V with composition (Xu et al. 2000)

In addition, in β-eucryptite Li induces a shortening of the O-O edges that are shared by the Li- and Si(Al)-tetrahedra in order to minimize Li-Si(Al) repulsion, distorting the framework tetrahedra (Tscherry and Schulz 1972b; Palmer 1994; Xu et al. 1999a). Upon heating, Li ions diffuse along the [0 0 1] channels and pass through the octahedral sites that are unoccupied at room temperature, causing an extension of the framework in the (0 0 1) plane and a contraction along c (Schulz 1974). Because the number of Li ions decreases with increasing x, the effect of Li disorder on thermal behavior becomes smaller. This may account for the slightly lower thermal anisotropy displayed by the phase with $x = 0.5$ in comparison with $x = 0.33$ (Fig. 2a, b), although they both have disordered structures.

The thermal behavior of the stuffed α-quartz phases ($x = 0.69$ and 0.9) is similar to that of pure α-quartz, except that the critical temperatures of their transitions to the β polymorphs are lower (Fig. 3a–c). The dominant mechanism responsible for the positive thermal expansion in these structures is a nearly rigid rotation of Si- or Al-tetrahedra around the ⟨1 0 0⟩ axes. The degree of tetrahedral rotation can be described by the tilt angle δ:

$$\tan\delta = 2\sqrt{3}/9(c/a)[(5-6z)/(1-x)] \quad , \qquad (1)$$

where a and c are lattice constants, and x and z are coordinates of oxygen (Grimm and Dorner 1975). As in pure α-quartz, with increasing temperature the tetrahedral tilt angle δ decreases approximately linearly in these stuffed derivatives (Fig. 5a). In addition, upon heating, the Si- or Al-tetrahedra may undergo a slight deformation involving a shortening parallel to c and a lengthening perpendicular to c, as in α-quartz (Grimm and Dorner 1975; Carpenter et al. 1998a). However, the effect of this tetrahedral deformation on the thermal behavior is relatively small.

As temperature exceeds T_c, the phase with $x = 0.69$ exhibits a much more pronounced contraction of the c-axis in comparison with the more siliceous compositions ($x = 0.9$ and quartz). On the other hand, the a-axis thermal variations are similar for all three compositions (Fig. 3a, b). This behavior is certainly related to the comparatively higher concentration of Li ions when $x = 0.69$, since Li ions tend to diffuse along the [0 0 1] structural channels on heating, and this process can result in a decrease in the cell dimension along c, as tetrahedral edges contract to minimize Li-(Al, Si) repulsion.

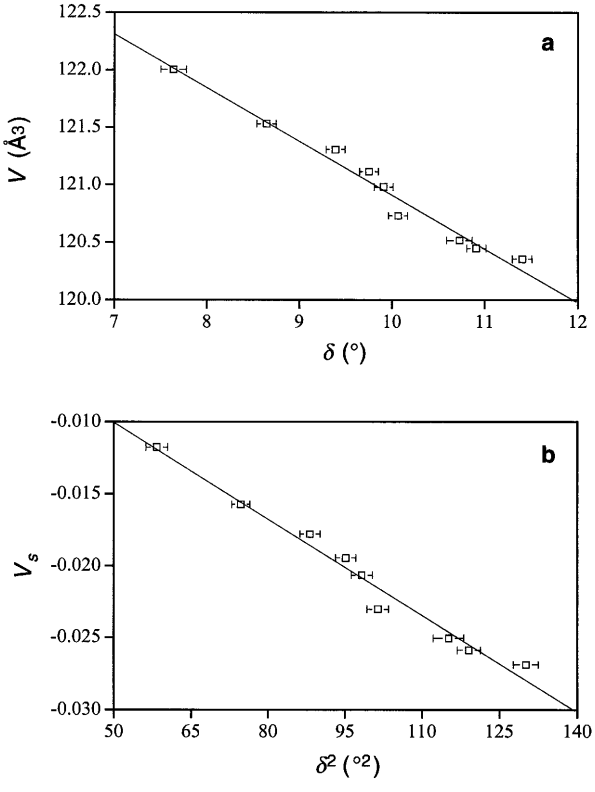

Fig. 5a, b Variation in cell volume V for the stuffed derivative of α-quartz $Li_{0.31}Al_{0.31}Si_{1.69}O_4$ as a function of the tetrahedral tilt angle δ^1. **b** Variation in volume strain V_s with δ^2

Effects of Li + Al → Si substitution on the α–β quartz transition

Critical temperature

A number of experimental studies have shown that impurities can change the critical temperatures of phase transitions (e.g., Keith and Tuttle 1952; Whatmore et al. 1978; Redfern 1992). For instance, Keith and Tuttle (1952) studied variations in the α–β quartz transition temperature in some natural and synthetic samples, and they attributed differences in T_c to small amounts of impurities and to disparities in crystal growth histories. Only recently, theoretical treatments based on a Landau-type mean field analysis have achieved significant success in describing the effects of impurities on phase transitions (Salje et al. 1991; Salje 1995). Salje et al.'s study demonstrates that the rate of change in T_c increases with increasing impurity content (N), and four distinct regimes are identified in terms of the magnitude of $\partial T_c/\partial N$. In particular, when the impurity concentration N greatly exceeds 10^{23} cm^{-3}, T_c becomes strongly dependent on N and varies linearly with N.

Figure 6 reveals the change in the α–β transition temperature with composition for the $Li_{1-x}Al_{1-x}Si_{1+x}O_4$ series. Critical temperatures for samples with composition $x = 0.69$, 0.9, and 1 were obtained using differential scanning calorimetry (Fig. 7). As can be seen in Fig. 6, the calorimetrically determined transition temperatures for these three compositions vary linearly as a function of the dopant concentration, $1 - x$: T_c (in K) = 836.5 – 1603.2($1 - x$). Although additional data for low dopant concentrations are desirable, the strong linear relationship between T_c and $(1 - x)$ for $0 \le (1 - x) \le 0.5$ suggests that the plateau effects described by Salje (1995) are small for this system.

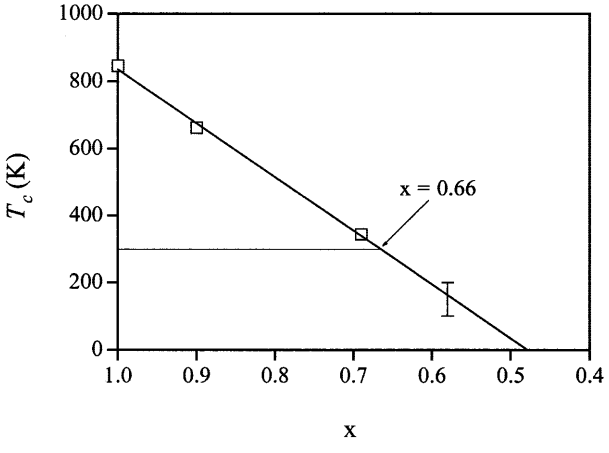

Fig. 6 Dependence of critical temperature T_c on (Li + Al) substitution in $Li_{1-x}Al_{1-x}Si_{1+x}O_4$. The *straight line* is a least-squares fit to the data for compositions $x = 0.69$, 0.9, and 1. *Brackets* represent the temperature range over which the secondary phase ($x = \sim 0.58$) in the sample with $x = 0.5$ undergoes the α–β quartz-like transition

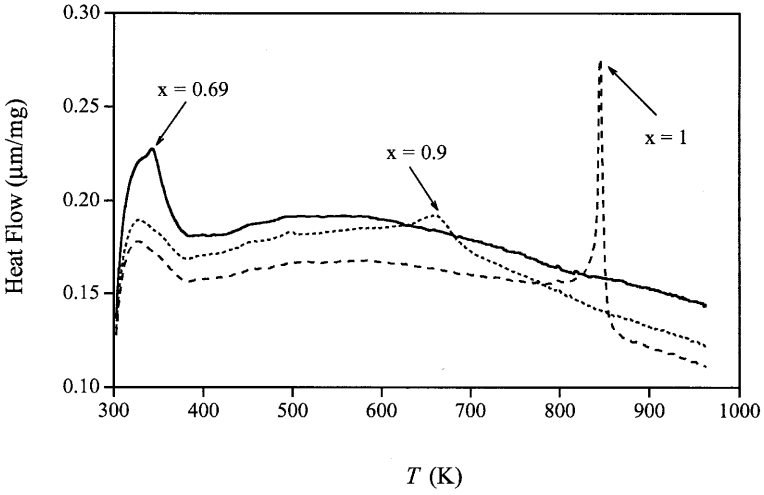

Fig. 7 Differential scanning calorimetry profiles for the $Li_{1-x}Al_{1-x}Si_{1+x}O_4$ phases with $x = 0.69$, 0.9 and 1. *Arrows* indicate α–β quartz-like transitions

Extrapolation of the $T_c - x$ dependence to 298 K suggests that $Li_{1-x}Al_{1-x}Si_{1+x}O_4$ will invert from an α- to a β-quartz-like structure at room temperature when $x = \sim 0.66$ (Fig. 6). This value is in good agreement with the critical composition of $x = \sim 0.65$, as was independently determined by our analysis of the relations between composition and room-temperature lattice parameters of $Li_{1-x}Al_{1-x}Si_{1+x}O_4$ (Xu et al. 2000). Although our synchrotron X-ray data (Fig. 4) do not allow us to pinpoint with high accuracy the α–β transition temperature and the composition for the secondary phase in the sample with bulk composition $x = 0.5$, the temperature range over which its α–β transitions must occur is fully consistent with the observed linear relationship when the $T_c - x$ dependence is extrapolated below 298 K (Fig. 6). Consequently, our results suggest that the α–β critical temperature varies linearly from 846 K to near 0 K as a function of increasing dopant concentration.

Spontaneous strain

Spontaneous strain has been used extensively to describe lattice distortions accompanying phase transitions (Salje 1990; Carpenter et al. 1998b). Because the strain is manifested as departures of cell dimensions from their idealized high-symmetry values, the spontaneous strain is measured using high-temperature dimensions extrapolated to the low-temperature regime (Schlenker et al. 1978; Redfern and Salje 1987). Since stuffed derivatives of α- and β-quartz have trigonal and hexagonal symmetries, respectively, and since their unit cells have coincident settings, there are, in addition to the volume strain $V_s = V/V_0 - 1$, only three nonzero elements in the strain tensor: $e_1 = e_2 = a/a_0 - 1$; $e_3 = c/c_0 - 1$, where a, c, and V are parameters of the α modification at a given temperature, and a_0, c_0 and V_0 are idealized parameters determined by extending high-temperature lattice variations into the stability field of the α polymorph (Carpenter et al. 1998a).

Table 2 Unit-cell parameters of the stuffed quartz-derivative phase $Li_{0.31}Al_{0.31}Si_{1.69}O_4$ as a function of temperature (determined from laboratory X-ray data)

T (K)	a (Å)	c (Å)	V (Å^3)
313	5.0927(2)	5.4498(3)	122.408(10)
333	5.0992(2)	5.4520(3)	122.768(10)
353	5.1079(2)	5.4553(3)	123.265(11)
373	5.1095(2)	5.4552(3)	123.336(11)
393	5.1097(2)	5.4548(3)	123.341(11)
413	5.1102(2)	5.4541(3)	123.350(11)
433	5.1103(2)	5.4540(3)	123.349(11)
453	5.1105(2)	5.4529(3)	123.336(11)
473	5.1104(2)	5.4523(3)	123.316(11)
493	5.1107(2)	5.4518(3)	123.318(11)
513	5.1106(2)	5.4509(3)	123.294(11)
533	5.1107(2)	5.4505(3)	123.289(10)
553	5.1106(2)	5.4497(3)	123.265(10)
573	5.1105(2)	5.4490(3)	123.246(11)
593	5.1104(2)	5.4483(3)	123.226(10)
613	5.1103(2)	5.4481(3)	123.218(10)
633	5.1101(2)	5.4476(3)	123.192(10)
653	5.1099(2)	5.4468(3)	123.164(10)
673	5.1100(2)	5.4464(3)	123.161(10)
693	5.1096(2)	5.4460(3)	123.134(10)
713	5.1093(2)	5.4457(3)	123.114(10)
733	5.1093(2)	5.4447(3)	123.091(10)
753	5.1092(2)	5.4448(3)	123.088(10)
773	5.1093(2)	5.4437(3)	123.071(10)
823	5.1088(2)	5.4428(3)	123.023(10)

A comparison of the thermally induced spontaneous strain associated with a partially stuffed derivative of quartz ($Li_{0.31}Al_{0.31}Si_{1.69}O_4$) with the strain of the pure end member (SiO_2) quantitatively reveals the extent to which Li + Al substitution can act as a proxy for temperature. Extrapolations of a_0, c_0 and V_0 of $Li_{0.31}Al_{0.31}Si_{1.69}O_4$ from linear regressions of the data above T_c can be described by a_0 (Å) $= 5.1121 - 3.64 \times 10^{-6}\ T$, c_0 (Å) $= 5.4656 - 2.82 \times 10^{-5}\ T$, and V_0 (Å^3) $= 123.699 - 8.15 \times 10^{-4}\ T$ (Table 2; Fig. 8). The calculated spontaneous strains (Fig. 9) can be fitted, to a good approximation, by the relation e_1 (or e_3 or V_s) $= A(T_c - T)^{1/2}$, where A is a constant and T_c is the

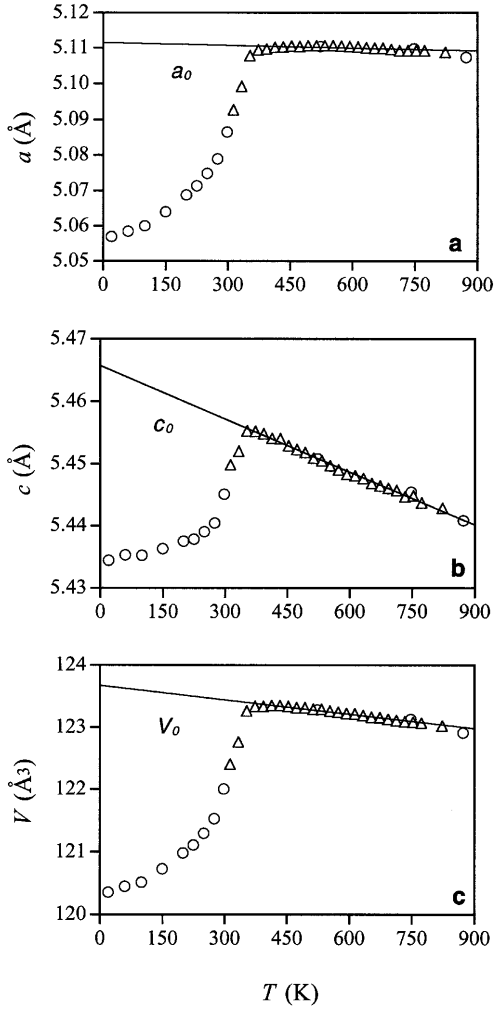

Fig. 8a–c Temperature dependence of the lattice parameters **a** a, **b** c, and **c** V for $Li_{0.31}Al_{0.31}Si_{1.69}O_4$ from synchrotron X-ray data (*circles*) and CuKα X-ray data (*triangles*). *Lines* indicate extrapolations of the data for the high-temperature β polymorph into the stability field of the α polymorph

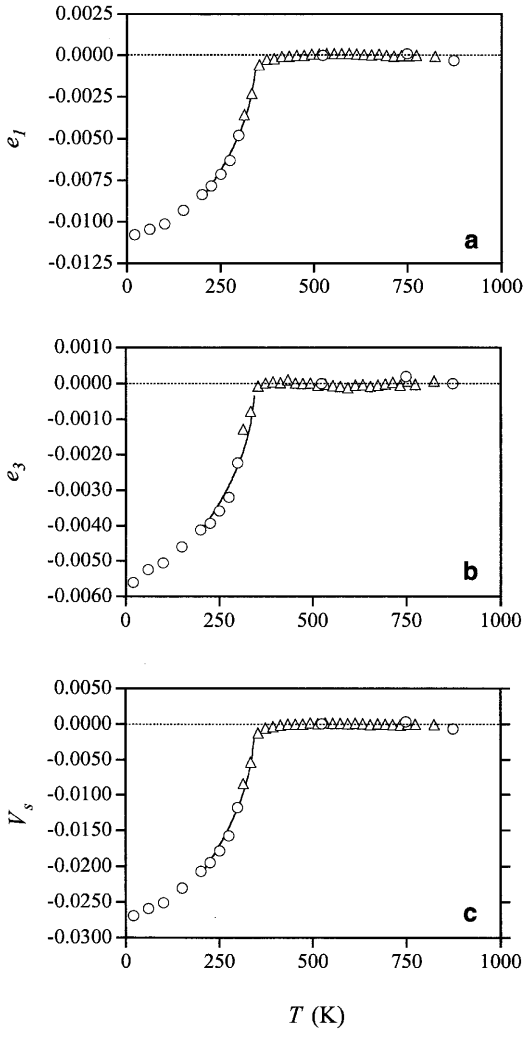

Fig. 9a–c Temperature dependence of the spontaneous strains **a** e_1, **b** e_3, and **c** V_s for $Li_{0.31}Al_{0.31}Si_{1.69}O_4$ (*symbols* as in Fig. 8). The *curves* are fits to the data with 200 K $\leq T \leq T_c$ using the equation e_1 (or e_3 or V_s) $= A(T_c - T)^{1/2}$, where A is a constant, and T_c is the critical composition of the α–β transition, which was determined to be 343 K from the DSC measurement shown in Fig. 7. The values of A for e_1, e_3, and V_s are −0.0358, −0.0186, and −0.0873, respectively. Note that strain data with $T < 200$ K were not included for the fitting because of the effects of order parameter saturation (Salje et al. 1991). The *dotted lines* represent linear extrapolations of the data with $T \geq T_c$ into the stability field for $T < T_c$

critical temperature of the α–β transition. Moreover, the volume strain (V_s) appears to vary approximately linearly with the square of tilt angle (δ^2) (Fig. 5b). As δ can be considered to be the order parameter (Q) of the α–β transition (Grimm and Dorner 1975), V_s is close to being proportional to Q^2 as well. These relations all suggest that the α–β transformation in $Li_{0.31}Al_{0.31}Si_{1.69}O_4$ is very close to tricritical, as is the first-order α–β quartz transition (Carpenter et al. 1998a). However, the magnitudes of the spontaneous strains for the (Li + Al)-doped phase are much smaller than those for pure quartz; the values of e_1, e_2, and V_s for quartz at $T/T_c = 0.5$ are ~1.5, ~0.9, and ~4%, respectively (Carpenter et al. 1998b), whereas the corresponding values for the stuffed phase $x = 0.69$ are only ~0.87, ~0.43, and ~2.16%.

The spontaneous strain provides a precise measure of the degree of structural deformation in a material as the result of a phase transition. The substitution of Li + Al for Si diminishes the spontaneous strain in stuffed derivatives of α-quartz because Li inhibits full framework collapse and limits the degree of deformation. Consequently, the thermal energy required to effect the transition to the expanded β modification is lower with higher Li + Al concentrations, and the critical temperatures systematically decrease with increasing $(1 - x)$. Similar behavior has been observed in other framework silicates, such as feldspar (e.g., Kroll et al. 1980; Carpenter 1988; Redfern 1992; Zhang et al. 1996). For example, the substitution of K^+ for Na^+ in albite dramatically decreases the critical temperature of the $C2/m$–$C\bar{1}$ transition (Kroll et al. 1980; Zhang et al. 1996), presumably because the larger K^+ can more effectively sustain the expanded $C2/m$ structure and stabilize it at lower temperatures.

As noted in many studies on feldspar (e.g., Carpenter 1988; Salje 1990), the effects of ionic substitutions on displacive transitions also depend on the degree of Al/Si order. The Al/Si order–disorder strongly interacts with the displacive transition via strain coupling (Salje 1990; Redfern 2000), such that a decrease in Al/Si order in anorthite lowers the T_c of the $I\bar{1}$–$P\bar{1}$ transition and also changes its character from tricritical to second-order (Redfern 1992). Although stuffed derivatives of quartz ($Li_{1-x}Al_{1-x}Si_{1+x}O_4$) with $x \geq \sim 0.3$ do not possess Al/Si long-range order, the short-range Al/Si order might influence the nature of the displacive transition. This possibility requires further investigation. Moreover, since Li ions positionally disorder on heating, this process probably affects the α–β transition as well. As documented in previous transmission electron microscopy (TEM) studies (Heaney and Veblen 1991b; Xu and Heaney 1997), point defects such as interstitial ions in quartz appear to pin the positions of the Dauphiné twins that arise from the β–α transition. In addition, higher concentrations of interstitial Li might be expected to stabilize the twin boundaries and thereby to increase twin boundary densities by decreasing the mean domain size. These relationships require investigation by detailed TEM studies of the microstructures in the stuffed derivatives of quartz at different temperatures.

Acknowledgements We are grateful to D. Cox, P.M. Woodward, and D.M. Yates for assistance with synchrotron X-ray experiments, and to G.H. Beall for providing the $Li_{0.31}Al_{0.31}Si_{1.69}O_4$ sample. We also thank three anonymous reviewers for helpful comments and Dr. J. A. Tyburczy for editorial handling. This work was supported by the NSF grants no. EAR-9418031 and no. EAR-9706143 (to P.J.H.) and the 1996 and 1997 ICDD crystallography scholarships (to H.X.). Synchrotron X-ray diffraction was carried out at the National Synchrotron Light Source (NSLS), Brookhaven National Laboratory, which is supported by the US Department of Energy, Division of Material Sciences and Division of Chemical Sciences. The calorimetry was performed at the UC-Davis Thermochemistry Facility, supported by CHiPR.

References

Beall GH (1994) Industrial applications of silica. In: Heaney PJ, Prewitt CT, Gibbs GV (eds) Silica. Rev Mineral, vol. 29 Mineral Soc Am, Washington, DC, pp 468–505

Buerger MJ (1954) The stuffed derivatives of the silica structures. Am Mineral 39: 600–614

Carpenter MA (1988) Thermochemistry of aluminum/silicon ordering in feldspar minerals. In: Salje EKH (ed) Physical properties and thermodynamic behavior of minerals. NATO ASI C, 225, Reidel, Dordrecht, pp 265–323

Carpenter MA (1992) Thermodynamics of phase transitions in minerals: a macroscopic approach. In: Price GD, Ross NL (eds) The stability of minerals. Chapman & Hall, London, pp 172–215

Carpenter MA, Salje EKH, Graeme-Barber A, Wruck B, Dove MT, Knight KS (1998a) Calibration of excess thermodynamic properties and elastic constant variations associated with the $\alpha \leftrightarrow \beta$ phase transition in quartz. Am Mineral 83: 2–22

Carpenter MA, Salje EKH, Graeme-Barber A (1998b) Spontaneous strain as a determinant of thermodynamic properties for phase transitions in minerals. Eur J Mineral 10: 621–691

Cox DE, Toby BH, Eddy MM (1988) Acquisition of powder diffraction data with synchrotron radiation. Aust J Phys 41: 117–131

Finger LW, Cox DE, Jephcoat AP (1994) A correction for powder diffraction peak asymmetry due to axial divergence. J Appl Crystallogr 27: 892–900

Gillery FH, Bush EA (1959) Thermal contraction of β-eucryptite (of $Li_2O{\cdot}Al_2O_3{\cdot}2SiO_2$) by X-ray and dilatometer methods. J Am Ceram Soc 42: 175–177

Grimm H, Dorner B (1975) On the mechanism of the α–β phase transformation of quartz. J Phys Chem Solids 36: 407–413

Guth H, Heger G (1979) Temperature dependence of the crystal structure of the one-dimensional Li^+-conductor β-eucryptite ($LiAlSiO_4$). In: Vashista P, Mundy JN, Shenoy GK (eds) Fast ion transport in solids. Elsevier, Amsterdam, pp 499–502

Heaney PJ (1994) Structure and chemistry of the low-pressure silica polymorphs. In: Heaney PJ, Prewitt CT, Gibbs GV (eds) Silica. Rev Mineral, vol. 29. Mineral Soc Am, Washington, DC, pp 1–40

Heaney PJ (2000) Phase transitions induced by solid solution. In: Redfern SAT, Carpenter MA (eds) Transformation processes in minerals. Rev Mineral, vol. 39. Mineral Soc Am, Washington, DC, pp 135–174

Heaney PJ, Veblen DR (1991a) Observation of the α–β transition in quartz: a review of imaging and diffraction studies and some new results. Am Mineral 76: 1018–1032

Heaney PJ, Veblen DR (1991b) Observation and kinetic analysis of a memory effect at the α–β quartz transition. Am Mineral 76: 1459–1466

Keith ML, Tuttle OF (1952) Significance of variance in high–low inversion of quartz. Am J Sci 253a: 203–280

Kroll H, Bambauer HU, Schirmer U (1980) The high albite–monalbite and analbite–monalbite transitions. Am Mineral 65: 1192–1211

Larson AC, Von Dreele RB (1994) GSAS – general structure analysis system. Los Alamos Nat Lab Rep LAUR 86–748, 179 p

Li CT (1968) The crystal structure of $LiAlSi_2O_6$ III (high-quartz solid solution). Z Kristallogr 127: 327–348

Lichtenstein AI, Jones RO, Xu H, Heaney PJ (1998) Anisotropic thermal expansion in the silicate β-eucryptite – a neutron diffraction and density functional study. Phys Rev (B) 58: 6219–6223

Müller G (1995) The scientific basis. In: Bach H (ed) Low thermal expansion glass ceramics. Springer Berlin Heidelberg New York, pp 13–49

Müller G, Hoffmann M, Neeff R (1988) Hydrogen substitution in lithium-aluminosilicates. J Mater Sci 23: 1779–1785

Müller WF (1979) The effect of heating on the domain structure of beta-eucryptite, $LiAlSiO_4$. J Mater Sci 14: 1433–1439

Palmer DC (1994) Stuffed derivatives of the silica polymorphs. In: Heaney PJ, Prewitt CT, Gibbs GV (eds) Silica. Rev Mineral, vol. 29. Mineral Soc Am, Washington, DC, pp 83–122

Petzoldt J (1967) Metastabile mischkristalle mit quarzstruktur mit oxidsystem Li_2O–MgO–ZnO–Al_2O_3–SiO_2. Glastechn Ber 40: 385–396

Pillars WW, Peacor DR (1973) The crystal structure of beta eucryptite as a function of temperature. Am Mineral 58: 681–690

Redfern SAT (1992) The effect of Al/Si disorder on the $I\bar{1}$–$P\bar{1}$ co-elastic phase transition in Ca-rich plagioclase. Phys Chem Miner 19: 246–254

Redfern SAT (2000) Order-disorder phase transitions. In: Redfern SAT, Carpenter MA (eds) Transformation processes in minerals. Rev Mineral, vol. 39. Mineral Soc Am, Washington, DC, pp 105–134

Redfern SAT, Salje EKH (1987) Thermodynamics of plagioclase: II. Temperature evolution of the spontaneous strain at the $I\bar{1}$–$P\bar{1}$ phase transition in anorthite. Phys Chem Miner 14: 189–195

Roy R (1995) Low thermal expansion ceramics: a retrospective. In: Stinton and Limaye (eds) Low-expansion materials. Ceramic transactions, vol. 52, Am Ceram Soc, pp 1–4

Salje EKH (1990) Phase transitions in ferroelastic and co-elastic crystals. Cambridge University Press, Cambridge

Salje EKH (1995) Chemical mixing and structural phase transitions: the plateau effect and oscillatory zoning near surfaces and interfaces. Eur J Mineral 7: 791–806

Salje EKH, Bismayer U, Wruck B, Hensler J (1991) Influence of lattice imperfections on the transition temperatures of structural phase transitions: the plateau effect. Phase Trans 35: 61–70

Schlenker JL, Gibbs GV, Boisen MB (1978) Strain-tensor components expressed in terms of lattice parameters. Acta Crystallogr A34: 52–54

Schulz H (1974) Thermal expansion of beta-eucryptite. J Am Ceram Soc 57: 313–317

Smith JV, Steele IM (1984) Chemical substitution in silica polymorphs. Neues Jahrb Min Mon 3: 137–144

Thompson P, Cox DE, Hastings J (1987) Rietveld refinement of Debye-Scherrer synchrotron X-ray data for Al_2O_3. J Appl Crystallogr 20: 79–83

Tscherry V, Schulz H, Laves F (1972) Average and super structure of β-eucryptite ($LiAlSiO_4$), Part II. Superstructure. Z Kristallogr 135: 175–198

Whatmore RW, Clarke R, Glazer AM (1978) Tricritical behavior in $PbZr_xTi_{1-x}O_3$ solid solutions. J Phys (C) Sol State Phys 11: 3089–3102

Will G, Bellotto M, Parrish W, Hart M (1988) Crystal structures of quartz and magnesium germanate by profile analysis of powder diffractometer data. J Appl Crystallogr 21: 182–191

Wright AF, Lehmann MS (1981) The structure of quartz at 25 and 590 °C determined by neutron diffraction. J Solid State Chem 36: 371–380

Xu H, Heaney PJ (1997) Memory effects of domain structures during displacive phase transitions: a high-temperature TEM study of quartz and anorthite. Am Mineral 82: 99–108

Xu H, Heaney PJ, Yates DM, Von Dreele RB, Bourke MA (1999a) Structural mechanisms underlying near-zero thermal expansion in β-eucryptite: A combined synchrotron X-ray and neutron Rietveld analysis. J Mater Res 14: 3138–3151

Xu H, Heaney PJ, Böhm H (1999b) Structural modulations and phase transitions in β-eucryptite: an in-situ TEM study. Phys Chem Miner 26: 633–643

Xu H, Heaney PJ, Navrotsky A, Topor L, Liu J (1999c) Thermochemistry of stuffed quartz-derivative phases along the join $LiAlSiO_4$–SiO_2. Am Mineral 84: 1360–1369

Xu H, Heaney PJ, Beall G (2000) Phase transitions induced by solid solution in stuffed derivatives of quartz: a powder synchrotron XRD study of the $LiAlSiO_4$–SiO_2 join. Am Mineral 85: 971–979

Zeyen CME, Dolino G, Bachheimer JP (1983) Neutron and calorimetric observation of a modulated structure in quartz just above the α–β phase transition. Physica 120(B): 280–282

Zhang M, Wruck B, Graeme-Barber A, Salje EKH, Carpenter MA (1996) Phonon spectra of alkali feldspars: phase transitions and solid solutions. Am Mineral 81: 92–104